The University of San Francisco
USF Scholarship: a digital repository @ Gleeson Library | Geschke Center

Physics and Astronomy | College of Arts and Sciences

2008

Controlled Compositional Disorder in Er3+:Y2SiO5 Provides a Wide-Bandwidth Spectral Hole Burning Material at 1.5mum

Thomas Böttger
University of San Francisco, tbottger@usfca.edu

C W. Thiel

R L. Cone

Y Sun

Follow this and additional works at: http://repository.usfca.edu/phys

 Part of the Physics Commons

Recommended Citation

Böttger, Thomas; Thiel, C. W.; Cone, R. L.; Sun, Y. Controlled compositional disorder in Er3+:Y2SiO5 provides a wide-bandwidth spectral hole burning material at 1.5mum. Phys. Rev. B 77, 155125 – Published 24 April 2008

This Article is brought to you for free and open access by the College of Arts and Sciences at USF Scholarship: a digital repository @ Gleeson Library | Geschke Center. It has been accepted for inclusion in Physics and Astronomy by an authorized administrator of USF Scholarship: a digital repository @ Gleeson Library | Geschke Center. For more information, please contact repository@usfca.edu.

Controlled compositional disorder in $Er^{3+}:Y_2SiO_5$ provides a wide-bandwidth spectral hole burning material at 1.5 μm

Thomas Böttger*
Department of Physics, University of San Francisco, 2130 Fulton Street, San Francisco, California 94117, USA and Department of Physics, Montana State University, Bozeman, Montana 59717, USA

C. W. Thiel† and R. L. Cone‡
Department of Physics, Montana State University, Bozeman, Montana 59717, USA

Y. Sun§
Department of Physics, Montana State University, Bozeman, Montana 59717, USA and Department of Physics, University of South Dakota, Vermillion, South Dakota 57069, USA

(Received 18 January 2008; published 24 April 2008)

The subgigahertz spectral bandwidth of the lowest energy 1.5 μm Er^{3+} $^4I_{15/2} \rightarrow {}^4I_{13/2}$ optical transition in $Er^{3+}:Y_2SiO_5$ has been increased to ~22 GHz by intentionally introducing compositional disorder through codoping with Eu^{3+} impurity ions. This illustrates a general bandwidth control technique for spectral hole burning device applications including spatial-spectral holography and quantum computing. Coherence measurements by stimulated photon echoes demonstrated that the increased disorder does not perturb the dynamical properties of the Er^{3+} transition and, thus, gives the desired bandwidth enhancement without penalty in other properties. The echo measurements and model analysis also show that phonon-driven spin flips of Er^{3+} ions in the ground state are responsible for the spectral diffusion that was observed for the optical transition. These results collectively give a better understanding of both the nature of disorder and of the ion-ion interactions in doped materials, and they also enable the high bandwidths required for signal processing and memory applications at 1.5 μm based on spectral hole burning.

DOI: 10.1103/PhysRevB.77.155125 PACS number(s): 42.50.Md, 76.30.Kg, 42.62.Fi, 78.40.−q

I. INTRODUCTION

One of the most challenging frontiers of optical materials research is the nature of disorder and its effect on optical properties. Disorder in optical materials spans a wide range from glasses to nearly perfect single crystals, with both dynamic and static disorders producing distinct effects on the optical properties. One of the emerging goals in the study of disorder in rare-earth-activated materials is to understand how controlled disorder may be introduced into nearly perfect crystals to enhance desirable material properties without producing negative consequences for other properties. Single crystals of Y_2SiO_5 doped with very low concentrations of rare-earth impurities are particularly well suited for this type of study. Previous work on Eu^{3+}-doped Y_2SiO_5 demonstrated how absorption spectroscopy combined with optical coherence measurements on rare-earth probe ions can detect and distinguish weak static and dynamic disorders in the host lattice.[1]

In this paper, we examine the effects of disorder on the properties of paramagnetic Er^{3+} ions in the Y_2SiO_5 host. The exceptionally narrow $Er^{3+}:Y_2SiO_5$ absorption linewidths of less than 500 MHz (or 0.02 cm^{-1}) and long coherence times greater than 4 ms, which correspond to a homogeneous linewidth of 73 Hz, provide particularly sensitive probes of static and dynamical aspects of the crystalline environment. The introduction of disorder through impurity doping to produce controlled modifications of the Er^{3+} linewidth demonstrates a level of material engineering that allows selective manipulation of properties desirable for device applications such as spatial-spectral holography (SSH).

The optical material $Er^{3+}:Y_2SiO_5$ is especially attractive for spectral hole burning (SHB) and SSH device applications, because it has resonant transitions with long fluorescence lifetimes and large oscillator strengths in the important 1.5 μm optical communications band,[2] and because it has narrow homogeneous linewidths and correspondingly long coherence lifetimes. The observed 73 Hz (Refs. 3 and 4) linewidth is one of the narrowest homogeneous optical transitions yet reported in a solid. Numerous proof-of-principle SSH/SHB demonstrations have been carried out in $Er^{3+}:Y_2SiO_5$, which are motivated by the desire to enable all-optical memory, switching, and processing,[5–8] and, more recently, quantum computing applications. This material has also been exploited as a laser frequency reference providing subkilohertz laser frequency stability, which is required for some of the aforementioned applications.[4,9–11]

Among the important material parameters for SSH/SHB applications are the homogeneous linewidth Γ_h, which determines or limits the potential frequency resolution, the inhomogeneous linewidth Γ_{inh}, which determines the signal processing bandwidth, and the ratio Γ_{inh}/Γ_h, which specifies the achievable time-bandwidth product. Previously, high-bandwidth applications were predominantly carried out in 0.1% $Tm^{3+}:Y_3Al_5O_{12}$ by using the Tm^{3+} transition located at 793.38 nm (vacuum) with $\Gamma_{inh} \sim 17$ GHz and $\Gamma_h \sim 4.2$ kHz.[8,12] While $Tm^{3+}:Y_3Al_5O_{12}$ possesses many favorable material parameters for wide-band optical processing, the 793 nm transition does not fall within a major telecommunication band where inexpensive components are available in mass production. The material $Er^{3+}:Y_2SiO_5$, on the

 ©2008 The American Physical Society

other hand, has favorable absorptions at 1.5 μm and exhibits extremely narrow homogeneous linewidths, but until now the achievable processing bandwidth in $Er^{3+}:Y_2SiO_5$ SSH demonstrations is limited by its inhomogeneous linewidths of typically less than 0.5 GHz.[2,6] The work reported here demonstrates that the inhomogeneous linewidth can be increased by introducing disorder while preserving the homogeneous linewidth and other desirable properties.

II. EXPERIMENT

Weak disorder was deliberately introduced into Er^{3+}-doped Y_2SiO_5 single crystals by codoping Eu^{3+} ions at 1 and 2 at. % concentrations into separate Czochralski growths of $0.02\%Er^{3+}:Y_2SiO_5$. The Eu^{3+} ions were chosen because they have no optical transitions in the region of interest and have a nonmagnetic $^7F_0$ ground state[13,14] so that minimal magnetic dipole interaction is expected. The Eu^{3+} ions simply substitute for the same-charge Y^{3+} host ions and, due to the very slightly different ionic radii, weakly perturb the ion spacings and, consequently, the crystal field level energies of Er^{3+} ions.

All samples were oriented, cut, and optically polished perpendicular to the three optical extinction axes[15] and held in an Oxford SpectroMag cryostat. Extreme care was taken in crystal alignments as well as in monitoring of the temperature and magnetic field strength. Slight crystal misalignments of less than 1° can cause a measurable effect on the coherence properties and lead to some variation in the results between the samples.

The laser source was a home-made Littman–Metcalf external cavity diode laser with a continuous mode-hop-free tuning range of ~40 GHz. Absorption experiments were carried out at $T=5$ K by using a collimated laser beam with a waist radius w_0 of 0.8 mm and an optical power of ~5 μW at the sample. The laser beam propagated parallel to the **b** axis of the crystal, and the electric field vector **E** of the light was chosen to be parallel to either the $\mathbf{D}_1$ or $\mathbf{D}_2$ extinction axis of the crystal. The laser-absorption spectra were measured by tuning the laser with a chirp rate of ~1 MHz/μs and detecting the transmission through the crystal with a 125 MHz InGaAs photodiode. Reference transmission spectra without the crystal were measured to correct the absorption data for laser intensity variations and interference fringes. The transmission spectrum of a fiber Fabry–Pérot interferometer with a 49.5 MHz free spectral range was simultaneously recorded with every laser-absorption spectrum to provide a convenient comb of frequency markers over the entire scan to allow for a precise calibration of the frequency scale and to correct for any small nonlinearities in the laser scan.[16] The absolute frequencies of the $0.02\%Er^{3+}:Y_2SiO_5$ absorption lines were determined by using a Burleigh WA-1500 wave meter that was calibrated to an absolute accuracy of better than ±50 MHz using a NIST traceable $H^{13}C^{14}N$ gas cell with a pressure of 10 Torr.[17] The individual $0.02\%Er^{3+}:1\%Eu^{3+}:Y_2SiO_5$ and $0.02\%Er^{3+}:2\%Eu^{3+}:Y_2SiO_5$ laser-absorption spectra were recorded simultaneously with $0.02\%Er^{3+}:Y_2SiO_5$ spectra in a dual beam experiment to provide absolute frequency calibration against the known $0.02\%Er^{3+}:Y_2SiO_5$ spectrum.

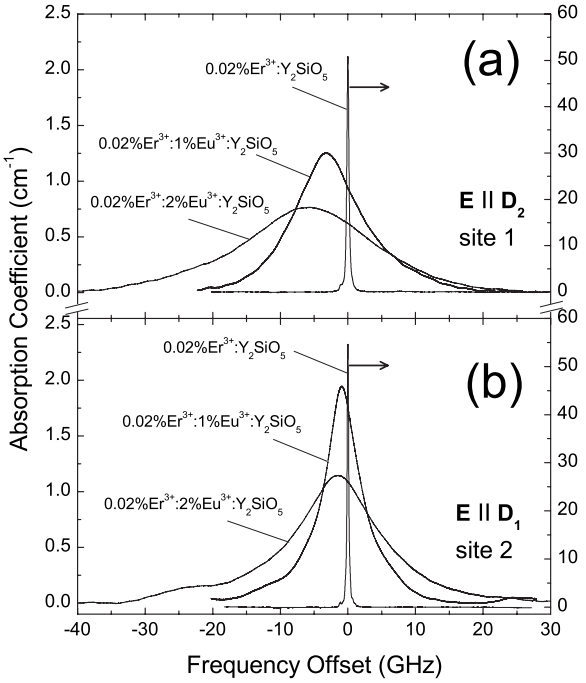

FIG. 1. Laser-absorption spectra with $\mathbf{k}\|\mathbf{b}$ at $T=5$ K in $0.02\%Er^{3+}:Y_2SiO_5$, $0.02\%Er^{3+}:1\%Eu^{3+}:Y_2SiO_5$, and $0.02\%Er^{3+}:2\%Eu^{3+}:Y_2SiO_5$ (a) polarized $\mathbf{E}\|\mathbf{D}_2$ for site 1 and (b) polarized $\mathbf{E}\|\mathbf{D}_1$ for site 2. Note that the frequency axis has been referenced to the peak absorption of $0.02\%Er^{3+}:Y_2SiO_5$ and the absorption coefficient for $0.02\%Er^{3+}:Y_2SiO_5$ is given on the right vertical axis.

Stimulated photon echo spectroscopy was used to study the influence of the Eu^{3+} impurity ion on the dynamic properties of the Er^{3+} optical center by measuring the decoherence of the Er^{3+} ions. The echo measurements were concentrated on site 1 and were carried out as a function of magnetic field at $T=1.6$ K. For these measurements, the crystals were aligned with $\mathbf{E}\|\mathbf{D}_2$, $\mathbf{B}\|\mathbf{D}_1$, and $\mathbf{k}\|\mathbf{b}$, and the experimental details followed those described in Ref. 18. Stimulated photon echo decays were recorded as a function of the separation t_{12} between the first and second pulses, with the waiting time T_W between the second and third pulses varied for each decay.

III. LASER-ABSORPTION SPECTROSCOPY

Typical laser-absorption spectra for crystals of each composition are shown in Fig. 1(a) for site 1 with the strongest absorption occurring for $\mathbf{E}\|\mathbf{D}_2$, and in Fig. 1(b) for site 2 with the strongest absorption occurring for $\mathbf{E}\|\mathbf{D}_1$. Note that the frequency axis is referenced to the peak absorption of the $0.02\%Er^{3+}:Y_2SiO_5$ crystal and that the absorption coefficient for $0.02\%Er^{3+}:Y_2SiO_5$ is given on the right vertical axis.

Inhomogeneous broadening of the Er^{3+} transitions results from the static disorder introduced into the crystalline environment by the random distribution of Eu^{3+} impurities located at Y^{3+} sites. The random distribution of impurity point

TABLE I. Measured material parameters describing laser absorption with $\mathbf{k}\|\mathbf{b}$ for the Er^{3+} $^4I_{15/2}$ to $^4I_{13/2}$ transition at site 1 with $\mathbf{E}\|\mathbf{D}_2$ and site 2 with $\mathbf{E}\|\mathbf{D}_1$. The frequency shift is measured with respect to the $0.02\%Er^{3+}:Y_2SiO_5$ crystal, with the site 1 line center measured at $195\,116.71\pm0.05$ GHz and site 2 at $194\,809.15\pm0.05$ GHz.

Material	Site 1, $\mathbf{E}\|\mathbf{D}_2$			Site 2, $\mathbf{E}\|\mathbf{D}_1$		
	Frequency shift (GHz)	Γ_{inh} (GHz)	α (cm^{-1})	Frequency shift (GHz)	Γ_{inh} (GHz)	α (cm^{-1})
$0.02\%Er^{3+}:Y_2SiO_5$	0	0.34	50	0	0.26	55
$0.02\%Er^{3+}:1\%Eu^{3+}:Y_2SiO_5$	−3.0	11	1.3	−0.9	6.0	1.9
$0.02\%Er^{3+}:2\%Eu^{3+}:Y_2SiO_5$	−6.0	22	0.76	−1.7	14	1.2

defects should produce a Lorentzian broadening of the absorption lines directly proportional to the impurity concentration,[19] but the magnitude of the broadening is determined by the nature of the interaction with the Er^{3+} ions. The most important mechanism leading to interactions between Eu^{3+} and Er^{3+} is presumably the localized strain in the host lattice and the modulation of the ion spacing due to the ionic radius mismatch between Eu^{3+} and Y^3. For the trivalent ions, there is an effective ionic radius difference between Eu^{3+} and Y^{3+} of 0.047 Å, while there is only a difference of 0.015 Å between Er^{3+} and Y^{3+}.[20] Another possible mechanism for the increase in the Er^{3+} inhomogeneous linewidth is an electric dipole-dipole interaction between Eu^{3+} and Er^{3+} ions.[21] Further measurements of the broadening of the Er^{3+} transitions by doping with other impurity ions are required to unambiguously determine the nature of the interaction mechanism.

All absorption lines were observed to be well described by Lorentzian line shapes, as expected.[19] A weak structure was observed in the tails of the $0.02\%Er^{3+}:Y_2SiO_5$ spectra due to partially resolved hyperfine transitions[22] of the naturally occurring ^{167}Er isotope. Other weak features in the tails of the Eu^{3+}-doped samples may result from the small number of Er^{3+} ions, with Eu^{3+} impurities occupying nearest neighbor or next-nearest neighbor lattice sites. For site 1, the absorption for $\mathbf{E}\|\mathbf{D}_1$ was 50% lower in all crystals compared to $\mathbf{E}\|\mathbf{D}_2$.[2] For site 2, the absorption for $\mathbf{E}\|\mathbf{D}_2$ was ten times lower compared to $\mathbf{E}\|\mathbf{D}_1$.[2] The lower peak absorption in $0.02\%Er^{3+}:2\%Eu^{3+}:Y_2SiO_5$—a consequence of the line broadening—led to a greater uncertainty in the measured absorption coefficients for both sites in that crystal. We found that the lowest energy Er^{3+} $^4I_{15/2}\rightarrow{}^4I_{13/2}$ ground state absorptions in $0.02\%Er^{3+}:Y_2SiO_5$ occur at 1536.4776 ± 0.0004 nm for site 1 and at 1538.9034 ± 0.0004 nm for site 2 in vacuum with the corresponding frequency values of 195116.71 ± 0.05 GHz and 194809.15 ± 0.05 GHz, respectively. These measurements provide improved accuracy over previously published values.[2,3] Transition frequencies for all samples were obtained by fitting the absorption profiles and are given as frequency shifts relative to the $0.02\%Er^{3+}Y_2SiO_5$ sample in Table I. We observed a line shift to lower frequency of 3 GHz per percent Eu^{3+} (900 MHz per percent Eu^{3+}) for site 1 (site 2), presumably due to the effect of the Eu^{3+} ions on the mean ionic spacings and the resultant change in local crystal field energies experienced by the Er^{3+} ions, as noted above. The measured peak absorption coefficients and linewidths for all crystals are listed in Table I. For site 1, the full-width at half-maximum (FWHM) of the inhomogeneous line is 0.34 GHz for $0.02\%Er^{3+}:Y_2SiO_5$, increasing to 11 GHz by codoping with 1 at. % Eu^{3+} and 22 GHz by codoping with 2 at. % Eu^{3+}. This corresponds to an ~11 GHz broadening per percent Eu^{3+} doping. For site 2, the FWHM of the inhomogeneous line is 0.26 GHz for $0.02\%Er^{3+}:Y_2SiO_5$, increasing to 6 GHz by codoping with 1 at. % Eu^{3+} and 14 GHz by codoping with 2 at. % Eu^{3+}, which corresponds to an ~6 GHz broadening per percent Eu^{3+} doping. The effect on Er^{3+} crystal field energies of Eu^{3+} impurities substituting for Y^{3+} ions is much larger than the effect of other Er^{3+} impurities substituting for Y^{3+} ions. In previous studies, we observed that the concentration broadening due to these lattice-strain-induced Er^{3+}-Er^{3+} interactions was ~1.6 GHz per percent Er^{3+} doping for site 1 in this material.[23] For the Er^{3+} concentrations of 0.02% investigated here, the Er^{3+} doping has a negligible effect on the absorption linewidths. These results may be contrasted with previous studies of the effect of Eu^{3+} concentration on the Eu^{3+} $^7F_0\rightarrow{}^5D_0$ transition linewidth in $Eu^{3+}:Y_2SiO_5$, where a larger broadening of 20 GHz per percent Eu^{3+} was observed.[13]

IV. STIMULATED PHOTON ECHO SPECTROSCOPY

While studying absorption spectra provides an accurate picture of the total effect of disorder on the impurity ion, more advanced nonlinear methods are required to distinguish between the effects of dynamic and static disorders. To determine if the Eu^{3+} impurity doping resulted in any dynamic disorder through localized structural fluctuations (two-level systems) or modulated ion-ion interactions, the optical dephasing of the Er^{3+} ion was probed over a wide range of time scales by using stimulated photon echo spectroscopy. The evolution of the linewidth with time provided by these measurements also led to insight into the microscopic Er^{3+} electron spin dynamics by measuring the effect of spectral diffusion on the homogeneous linewidth and isolating the different contributions to dephasing and ion-ion interactions.[18]

Stimulated echo decays were fitted to the generalized echo decay function given by Eq. (3) in Ref. 18 from which a time-dependent effective linewidth Γ_{eff} (t_{12}, T_W) was extracted. The functional form for the effective linewidth as $t_{12} \rightarrow 0$ is given by

$$\Gamma_{\text{eff}}(T_W) = \Gamma_h + \tfrac{1}{2}\Gamma_{SD}[1 - \exp\{-RT_W\}], \tag{1}$$

where Γ_h is the linewidth in the absence of spectral diffusion, Γ_{SD} is the FWHM of the dynamic distribution of transition frequencies due to spectral diffusion (SD), and R is the characteristic rate of the spectral diffusion process. The field dependence of the spectral diffusion linewidth Γ_{SD} (B) was described by Er^{3+}-Er^{3+} magnetic dipole interactions between site 1 Er^{3+} ions and is given by

$$\Gamma_{SD}(B) = \Gamma_{\max} \operatorname{sech}^2\left(\frac{g_{\text{env}}\mu_B B}{2kT}\right), \tag{2}$$

where $\Gamma_{\max}$ is the FWHM of the frequency broadening in the high temperature or low field limit, g_{env} describes the g factor of the perturbing magnetic moments that are randomly distributed throughout the crystal lattice, μ_B is the Bohr magneton, and k is the Boltzmann constant. For the $\mathbf{B} \| \mathbf{D}_1$ direction, site 2 has a much larger ground state energy level splitting compared to site 1 and, hence, site 2 spin flips do not contribute to spectral diffusion for the magnetic fields and temperature studied in this work.[2] The field dependence of the spectral diffusion rate R was best described by the one-phonon direct process for spin-lattice relaxation involving absorption or emission of a single phonon resonant with the perturbing moment's spin-flip transition and is given by

$$R(B) = R_0 + \alpha_D g_{\text{env}}^3 B^5 \coth\left(\frac{g_{\text{env}}\mu_B B}{2kT}\right), \tag{3}$$

where α_D is a generally anisotropic constant characterizing the strength of the phonon coupling and R_0 describes field-independent contributions to the spectral diffusion rate.

Results of the stimulated echo analysis are shown in Fig. 2 for (a) $0.02\%\,Er^{3+}:2\%\,Eu^{3+}:Y_2SiO_5$, (b) $0.02\%\,Er^{3+}:1\%\,Eu^{3+}:Y_2SiO_5$, and (c) $0.02\%\,Er^{3+}:Y_2SiO_5$, where the evolution of the effective linewidth is mapped as a function of T_W for a range of magnetic fields from 0.8 up to 3.1 T at 1.6 K. Solid lines in the figure are least-squares fits to the data using Eq. (1), with fitting parameters plotted in Fig. 3 and listed in Table II; note that Γ_h was averaged over all measured fields. Spectral diffusion was found in the broadening of the linewidth as T_W was increased; a plateau was observed after several hundred microseconds, where the contribution of spectral diffusion to the linewidth reached its full effect. Larger magnetic fields dramatically suppressed linewidth broadening due to an increase in magnetic order, which demonstrates how the magnetic field strength may be chosen to reduce the linewidth to a particular level required in a device application. The data of Fig. 2 confirm that codoping with Eu^{3+} ions did not affect the coherence properties of the Er^{3+} ions, as saturation levels were attained for all samples at identical fields and waiting times. The only noticeable difference between the samples was a slight increase in linewidth at the longest time scales and largest

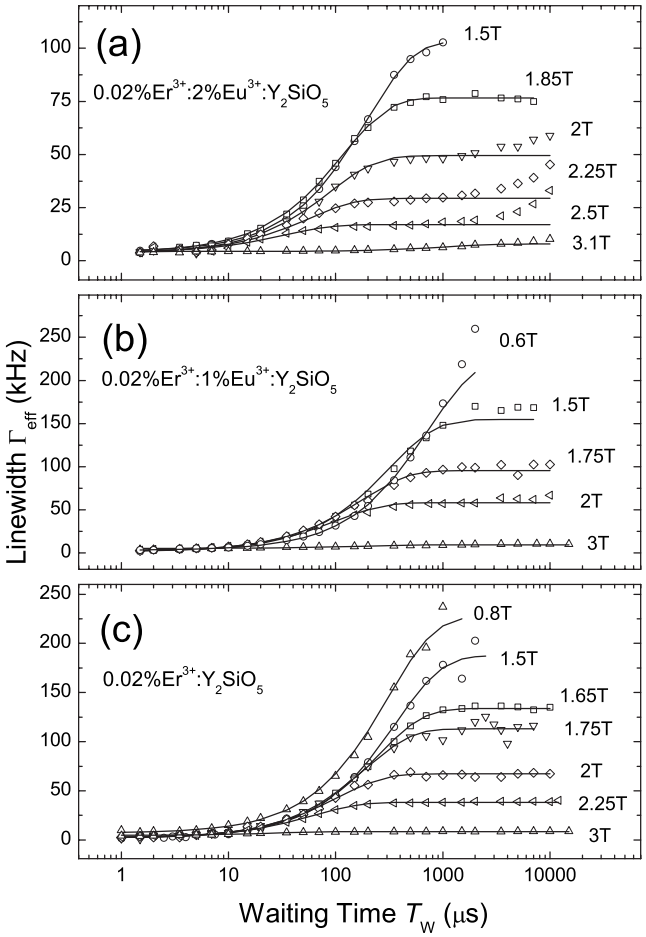

FIG. 2. Evolution of the effective linewidth for site 1 in (a) $0.02\%\,Er^{3+}:2\%\,Eu^{3+}:Y_2SiO_5$, (b) $0.02\%\,Er^{3+}:1\%\,Eu^{3+}:Y_2SiO_5$, and (c) $0.02\%\,Er^{3+}:Y_2SiO_5$ at 1.6 K as the waiting time T_W was changed. The magnetic field was varied over the range from $B = 0.8$ T to $B = 3.1$ T. Solid lines are least-squares fits to the data using Eq. (1).

magnetic fields measured for the sample doped with 2% Eu^{3+}. While this behavior may be an artifact due to the difficulty of measuring echo decays at the longest time scales studied due to laser frequency drift and weaker echo intensities, this effect could also indicate a small increase in ^{89}Y nuclear spin-flip rates with increased Eu^{3+} impurity concentration. This type of very slow spectral diffusion due to ^{89}Y-Er^{3+} interactions has been observed in $Er^{3+}:Y_2SiO_5$ over longer time scales,[18] and nuclear magnetic resonance measurements on other material systems have suggested that doping with Eu^{3+} impurities can increase the ^{89}Y spin-lattice relaxation rate.[24] While further measurements are required to determine if Eu^{3+} impurities may perturb the ^{89}Y spin dynamics in Y_2SiO_5, this weak effect would have no impact on the decoherence properties of Er^{3+} over the time scales of practical interest for device applications.

The consistency of the decoherence properties between the different samples is particularly apparent in Figs. 3(a) and 3(b), where the field-dependent linewidth saturation values $\Gamma_{\max}(B)$ and relaxation rates $R(B)$ obtained from the fits shown in Fig. 2 are plotted and all three crystals exhibit the

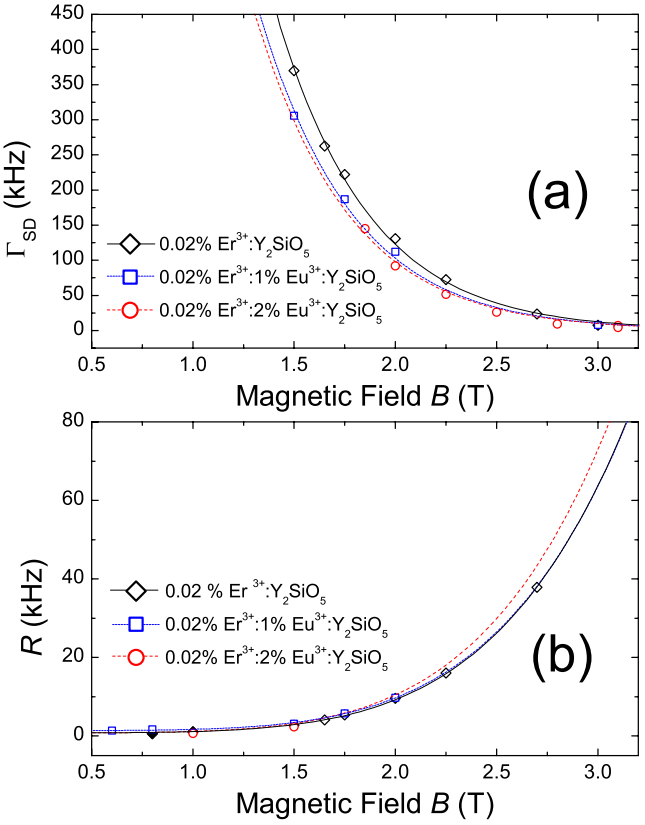

FIG. 3. (Color online) (a) Measured spectral diffusion linewidth Γ_{SD} and (b) relaxation rate R as a function of magnetic field for $0.02\%\,Er^{3+}:2\%\,Eu^{3+}:Y_2SiO_5$, $0.02\%\,Er^{3+}:1\%\,Eu^{3+}:Y_2SiO_5$, and $0.02\%\,Er^{3+}:Y_2SiO_5$ at 1.6 K. Solid symbols in (b) were estimated as described in the text. The lines are least-squares fits using Eqs. (2) and (3), respectively, with the parameters summarized in Table II.

same behavior. For lower fields where the maximum spectral diffusion broadening was not reached, estimates for R were obtained by using the experimental values of Γ_{max} and Eq. (2) to estimate Γ_{SD}, which allow R to be determined from fitting the data to Eq. (1) with Γ_{SD} held fixed at its extrapolated value. Values of R estimated by using this approach are indicated by solid symbols in Fig. 3(b). Furthermore, for cases where the spectral diffusion was completely suppressed at high fields, no R values can be extracted.

Lines in Fig. 3 are least-squares fits to the magnetic-field-dependent saturated linewidth $\Gamma_{max}(B)$ and rate $R(B)$ using Eqs. (2) and (3), respectively. Both fits gave excellent agreement for all three crystals, with fitting parameters summarized in Table II. Small deviations between the individual crystals can be attributed to slight crystal misalignments. It should be noted that the measured ground state g value of $g=5.5$ for site 1 with $\mathbf{B}\|\mathbf{D}_1$ was used for g_{env},[25] which clearly indicates that the spectral diffusion was dominated by spin flips of environmental Er^{3+} ions occupying site 1. The value of $g=5.5$ used in this work is more accurate than the value of 6.1 used in previous work,[3,18] but the small difference in values does not have a significant effect on the fit. Spin flips of Er^{3+} ions at site 2 were "frozen out" due to the much larger ground state energy level splitting for the $\mathbf{B}\|\mathbf{D}_1$ direction.[2] As expected, spectral diffusion was dramatically suppressed for larger magnetic fields, and the functional dependence of the rapidly increasing rate R with field unambiguously identified the direct-process phonon relaxation as the physical mechanism driving the spectral diffusion dynamics.

TABLE II. Measured material parameters describing optical decoherence and spectral diffusion for the $^4I_{15/2}$ to $^4I_{13/2}$ transition of Er^{3+} ions at site 1 for $\mathbf{B}\|\mathbf{D}_1$, $\mathbf{E}\|\mathbf{D}_2$, and $\mathbf{k}\|\mathbf{b}$ in $0.02\%\,Er^{3+}:Y_2SiO_5$, $0.02\%\,Er^{3+}:1\%\,Eu^{3+}:Y_2SiO_5$, and $0.02\%\,Er^{3+}:2\%\,Eu^{3+}:Y_2SiO_5$.

Material	α_D (kHz/T^5)	Γ_{max} (MHz)	R_0 (kHz)	Γ_h (kHz)
$0.02\%\,Er^{3+}:Y_2SiO_5$	1.1×10^{-3}	4.7	0.9	3.2
$0.02\%\,Er^{3+}:1\%\,Eu^{3+}:Y_2SiO_5$	1.1×10^{-3}	3.9	1.4	1.9
$0.02\%\,Er^{3+}:2\%\,Eu^{3+}:Y_2SiO_5$	1.3×10^{-3}	4.1	0.8	3.7

In some other material systems that we have studied, e.g., Tm-doped garnets with mixed Y and Lu host composition (which also involves no charge compensation), a similar increase in Γ_{inh} was also observed without increasing Γ_{hom}.[8] Many other cases are known, however, where the disorder that creates additional inhomogeneous broadening is accompanied by a departure from stoichiometry and dynamic disorder modes that cause an increased homogeneous broadening. Such materials include Pr^{3+} in cubic zirconia,[26] $Eu^{3+}:Y_2O_3$,[27] $Eu^{3+}:Y_2SiO_5$,[1] and $Pr^{3+}:LiNbO_3$.[28] What the present work demonstrated is that homogeneous broadening induced by disorder is an effect of specific growth conditions rather than an intrinsic property of doping itself, which confirmed what was seen in Ref. 1.

V. SUMMARY

The static and dynamical behaviors of $0.02\%\,Er^{3+}:Y_2SiO_5$ crystals codoped with 1 and 2 at. % Eu^{3+} ions have been characterized with laser absorption and stimulated photon echo spectroscopy. It was demonstrated that the signal processing bandwidth of the material can be dramatically extended from ~0.3 GHz up to several tens of gigahertz and perhaps more, making the material suitable for high-bandwidth SSH/SHB applications in the 1.5 μm communication band where devices can be particularly important and where inexpensive electro-optic components and fiber amplifiers reduce costs. The extensive stimulated photon echo data demonstrated that, while static transition frequencies were randomly shifted, producing the broadened absorption and, consequently, broader bandwidth for applications, the dynamical properties and spectral resolution of the Er^{3+} optical center were not affected by codoping with Eu^{3+} ions. The observed spectral diffusion was accurately described and predicted by spin flips of Er^{3+} ions at crystallographic site 1, which was driven by the direct-phonon process. This insight, coupled with detailed model projections, can now guide material design and selection of operating conditions that enhance the capabilities of SSH and SHB optical technologies and give a better understanding of both the nature of disorder and the ion-ion interactions in doped materials.

ACKNOWLEDGMENTS

The authors are grateful to R. W. Equall and R. L. Hutcheson of Scientific Materials Corporation of Bozeman, Montana for providing the crystals. This research was supported by AFOSR Grant No. F49620-00-1-0314 and DARPA Grant No. MDA972-03-1-0002. T.B. wishes to acknowledge financial support from the University of San Francisco Faculty Development Fund.

*Permanent address: Department of Physics, University of San Francisco, 2130 Fulton Street, San Francisco, California 94117, USA; tbottger@usfca.edu

†thiel@physics.montana.edu

‡cone@montana.edu

§Permanent address: Department of Physics, University of South Dakota, Vermillion, South Dakota 57069, USA; ycsun@usd.edu

[1] R. M. Macfarlane, Y. Sun, R. L. Cone, C. W. Thiel, and R. W. Equall, J. Lumin. **107**, 310 (2004).

[2] Thomas Böttger, C. W. Thiel, Y. Sun, and R. L. Cone, Phys. Rev. B **74**, 075107 (2006).

[3] Thomas Böttger, Y. Sun, C. W. Thiel, and R. L. Cone, Proc. SPIE **4988**, 51 (2003).

[4] Thomas Böttger, Ph.D. thesis, Montana State University, 2002.

[5] T. L. Harris, Y. Sun, W. R. Babbitt, R. L. Cone, J. A. Ritcey, and R. W. Equall, Opt. Lett. **25**, 85 (2000).

[6] Z. Cole, Thomas Böttger, R. Krishna Mohan, R. Reibel, W. R. Babbitt, R. L. Cone, and K. D. Merkel, Appl. Phys. Lett. **81**, 3525 (2002).

[7] V. Crozatier, G. Gorju, F. Bretenaker, J.-L. Le Gouët, and I. Lorgere, Opt. Lett. **31**, 3264 (2006).

[8] Y. C. Sun, in *Spectroscopic Properties of Rare Earths in Optical Materials*, edited by Guokui Liu and B. Jacquier (Springer-Verlag, Berlin, 2005), Chap. 7, pp. 379–429.

[9] P. B. Sellin, N. M. Strickland, T. Böttger, J. L. Carlsten, and R. L. Cone, Phys. Rev. B **63**, 155111 (2001).

[10] T. Böttger, Y. Sun, G. J. Pryde, G. Reinemer, and R. L. Cone, J. Lumin. **94-95**, 565 (2001).

[11] G. J. Pryde, Thomas Böttger, and R. L. Cone, J. Lumin. **94-95**, 587 (2001).

[12] M. Z. Tian, J. Zhao, Z. Cole, R. Reibel, and W. R. Babbitt, J. Opt. Soc. Am. B **18**, 673 (2001).

[13] F. Könz, Y. Sun, C. W. Thiel, R. L. Cone, R. W. Equall, R. L. Hutcheson, and R. M. Macfarlane, Phys. Rev. B **68**, 085109 (2003).

[14] R. W. Equall, Y. Sun, R. L. Cone, and R. M. Macfarlane, Phys. Rev. Lett. **72**, 2179 (1994).

[15] C. Li, C. Wyon, and Richard Moncorge, IEEE J. Quantum Electron. **28**, 1209 (1992).

[16] Data analysis software by C. W. Thiel.

[17] W. C. Swann and S. L. Gilbert, J. Opt. Soc. Am. B **22**, 1749 (2005).

[18] Thomas Böttger, C. W. Thiel, Y. Sun, and R. L. Cone, Phys. Rev. B **73**, 075101 (2006).

[19] A. M. Stoneham, Rev. Mod. Phys. **41**, 82 (1969).

[20] R. D. Shannon, Acta Crystallogr., Sect. A: Cryst. Phys., Diffr., Theor. Gen. Crystallogr. **32**, 751 (1976).

[21] M. J. Sellars, E. Fraval, and J. J. Longdell, J. Lumin. **107**, 150 (2004).

[22] O. Guillot-Noël, Ph. Goldner, Y. L. Du, E. Baldit, P. Monnier, and K. Bencheikh, Phys. Rev. B **74**, 214409 (2006).

[23] C. W. Thiel, Thomas Böttger, and R. L. Cone (unpublished).

[24] R. H. Meinhold and K. J. D. MacKenzie, Solid State Nucl. Magn. Reson. **5**, 151 (1995).

[25] Y. Sun, Thomas Böttger, C. W. Thiel, and R. L. Cone, Phys. Rev. B **77**, 085124 (2008).

[26] K. Tanaka, T. Okuno, Y. Yugami, M. Ishigami, and T. Suemoto, Opt. Commun. **86**, 45 (1991).

[27] G. P. Flinn, K. W. Jang, J. Ganem, M. L. Jones, R. S. Meltzer, and R. M. Macfarlane, J. Lumin. **58**, 374 (1994).

[28] R. M. Macfarlane, F. Könz, Y. Sun, and R. L. Cone, J. Lumin. **86**, 311 (2000).